Resource

Cell

Identification of Multipotent Luminal Progenitor Cells in Human Prostate Organoid Cultures

Wouter R. Karthaus,[1] Phillip J. Iaquinta,[2] Jarno Drost,[1] Ana Gracanin,[1] Ruben van Boxtel,[1] John Wongvipat,[2] Catherine M. Dowling,[2] Dong Gao,[2] Harry Begthel,[1] Norman Sachs,[1] Robert G.J. Vries,[1] Edwin Cuppen,[1] Yu Chen,[2] Charles L. Sawyers,[2,3] and Hans C. Clevers[1,*]

[1]Hubrecht Institute, Royal Netherlands Academy of Arts and Sciences and University Medical Center Utrecht, 3584 CT, Utrecht, Netherlands
[2]Human Oncology and Pathogenesis Program, Memorial Sloan Kettering Cancer Center, New York, NY 10065, USA
[3]Howard Hughes Medical Institute
*Correspondence: h.clevers@hubrecht.eu
http://dx.doi.org/10.1016/j.cell.2014.08.017

SUMMARY

The prostate gland consists of basal and luminal cells arranged as pseudostratified epithelium. In tissue recombination models, only basal cells reconstitute a complete prostate gland, yet murine lineage-tracing experiments show that luminal cells generate basal cells. It has remained challenging to address the molecular details of these transitions and whether they apply to humans, due to the lack of culture conditions that recapitulate prostate gland architecture. Here, we describe a 3D culture system that supports long-term expansion of primary mouse and human prostate organoids, composed of fully differentiated CK5+ basal and CK8+ luminal cells. Organoids are genetically stable, reconstitute prostate glands in recombination assays, and can be experimentally manipulated. Single human luminal and basal cells give rise to organoids, yet luminal-cell-derived organoids more closely resemble prostate glands. These data support a luminal multilineage progenitor cell model for prostate tissue and establish a robust, scalable system for mechanistic studies.

INTRODUCTION

The prostate is a male sex gland responsible for approximately 30% of all seminal fluid. Although prostate glands differ between species, macroscopically prostatic acini are organized similarly at the cellular level. Prostatic ducts are lined by a pseudostratified epithelium. Three major cell types are identified within the epithelium: (1) secretory luminal cells marked by cytokeratin (CK) 8, CK18, androgen receptor (AR) and secretory proteins like prostate-specific antigen (PSA); (2) basal cells, identified by the expression of CK5, CK14, and p63; and (3) rare neuroendocrine cells (Shen and Abate-Shen, 2010). In the developing and adult prostate, rare, intermediate cells expressing both luminal and basal markers are present (Hudson et al., 2001; Xue et al., 1998).

The identity of prostatic stem cells and how they give rise to these three cell types remains unclear. The classic urogenital sinus mesenchyme (UGSM) recombination model, where prostate epithelial cells are combined with mesenchymal cells derived from the urogenital sinus (UGS) of murine embryos and are transplanted under the kidney capsule (Cunha, 1973; Xin et al., 2003), suggests that only basal cells are capable of generating glandular tissue (Goldstein et al., 2008). Other approaches to identify prostate stem cells involve in vitro culture methods of primary prostate epithelium (Garraway et al., 2010; Liu et al., 2012; Niranjan et al., 2013). In these approaches, basal cells appear bipotent, i.e., capable of generating both luminal and basal lineages, indicating that basal cells have stem-like potential. However, none of these in vitro systems generate tissues that resemble the in vivo composition of the prostate gland or contain AR at physiological levels.

Recently, novel insights have been generated into the cellular hierarchy of the prostatic epithelium in mice through lineage tracing. Studies marking Ck5-expressing (Ck5+) basal cells and Ck8+ luminal cells suggest that basal and luminal lineages both harbor stem cell activity in the adult prostate (Choi et al., 2012; Ousset et al., 2012). However, in a separate study, rare multipotent basal cells reside in the adult prostate (Wang et al., 2013). While lineage tracing from Ck8+ and Ck18+ cells suggests unipotency in the luminal lineage (Choi et al., 2012; Ousset et al., 2012), a subset of luminal cells defined by Nkx3.1 expression postcastration can generate both lineages during regeneration of the prostate (Wang et al., 2009). Taken together, these studies suggest that in mice both luminal and basal cells sporadically are bipotent.

Although these studies provide important insights into prostate biology, translating these results to a human setting is difficult. One challenge is the expression pattern of the proposed stem cell markers c-kit, CD177, and CD133, which are exclusively expressed by basal cells in humans, but in mice are expressed by basal cells and a subset of luminal cells (Leong et al., 2008; Missol-Kolka et al., 2011). Translation to a human setting is also hampered by the lack of suitable human experimental systems.

We have previously described 3D culture conditions that allow long-term expansion of primary mouse and human epithelial

organoids from small intestine (Sato et al., 2009), colon (Sato et al., 2011), stomach (Barker et al., 2010), and liver (Huch et al., 2013). These cultures can be initiated from single Lgr5$^+$ stem cells and are based on the addition of the Lgr4/5 ligand R-spondin1, a potent Wnt pathway agonist (Binnerts et al., 2007; Carmon et al., 2011; de Lau et al., 2011). Organoids remain genetically and phenotypically stable in culture, exemplified by pathology-free transplantation of multiple mice with the organoid offspring of single Lgr5+ cells from colon (Yui et al., 2012) or liver (Huch et al., 2013).

Here, we describe the development of an R-spondin1-based culture method that allows long-term propagation of murine and human prostate epithelium. Using this method, we show that both basal and luminal populations contain bipotent progenitor cells, which retain full differentiation toward basal and luminal lineages in vitro and in the UGSM transplantation model. Moreover, we show that organoid cultures can be used to study prostate cancer initiation.

RESULTS

Establishment of Primary Murine Prostate Organoid Cultures with Basal and Luminal Epithelial Layers

To establish murine prostate organoid cultures, we embedded dissociated cells of wild-type murine prostate epithelium in Matrigel and added "generic" organoid medium containing the growth factors EGF, Noggin, and R-spondin1 (ENR) (Sato et al., 2009). We also included the Alk3/4/5 inhibitor A83-01 to inhibit TGF-β pathway signaling to prevent a proliferative block in prostate cells (Ding et al., 2011; Qin et al., 2013). Because the murine prostate is composed of different lobes with some distinct properties (Marker et al., 2003), we separately cultured the anterior prostate (AP), dorsolateral prostate (DLP), and ventral prostate (VP) epithelium (Figure S1A, available online). Prostate cells from each lobe yielded expanding organoids. These have been cultured at a split ratio of 1:3 for >1.5 years with stable, normal karyotypes (Figure S1B) and no changes in morphology.

Prostate epithelium formed cystic structures composed of a basal (outer) layer exclusively expressing typical basal prostate markers, such as p63 and Ck5, and a luminal (inner) layer exclusively expressing Ck8 (Figures 1A and 1B and S1D), thus demonstrating that organoids retain an architecture that resembles prostate glands in vivo, with the exception that we did not detect neuroendocrine cells.

Organoids also retained robust expression of the Ar (Figure 1A) and the prostate-specific transcription factor *Nkx3.1* (Figure S1C) (Bhatia-Gaur et al., 1999). Ar signaling was intact, as demonstrated by nuclear translocation of Ar in organoids treated with dihydrotestosterone (DHT). Within 72 hr after DHT addition, Ck8+ luminal cells became strongly polarized with an apparent increase in size (Figure 1A). Moreover, we found occasional double p63+ and Ar+ cells (Figure 1B), consistent with the differentiation-promoting function of Ar in normal prostate cells (Litvinov et al., 2006). Two classic Ar target genes, *Fkbp5* and *Psca*, were robustly upregulated (Figure 1D). DHT also enhanced the rate at which organoids expanded, allowing weekly split ratios of 1:5 rather than 1:3. Organoids also retained DHT responsiveness after multiple cycles of DHT addition and withdrawal (Figure S1E), consistent with the response of the normal prostate gland to castration and DHT add-back in vivo.

As has been shown for primary murine prostate tissue, prostate organoids gave rise to reconstituted prostate glands when placed under the kidney capsule with urogenital mesenchymal cells (Figure 1C, Figure S1J), using a tissue recombination assay (Xin et al., 2003). Importantly, this reconstitution property was retained after eight passages with organoids derived from the AP, DLP, or VP, indicating long-term retention of prostate progenitor cells. In the grafts, we did not observe morphologies reminiscent of the respective lobes of the prostate, suggesting that this is imparted by local, nonepithelial cues in the prostate as has been shown by others (Hayashi et al., 1993; Timms et al., 1995).

We examined the relative requirement of each ingredient by quantifying the number of organoids formed after seeding 1,000 single cells and tracking successive passages. Noggin increased the number of organoids formed during initial plating (Figure S1G) and resulted in faster expansion rates but was not absolutely required for serial passaging (Figure S1H). This is in line with observations in the development of the prostate in *Noggin* knockout mice, where reduced epithelial proliferation and reduced prostate budding is observed due to hyperactive bone morphogenetic protein (BMP) signaling (Cook et al., 2007). Similarly, the Wnt agonist R-spondin enhanced organoid formation and expansion, but was not absolutely required for expansion. R-spondins and Wnts are widely expressed in the urogenital sinus during prostate development (Mehta et al., 2011), and Wnt signaling is essential for prostate development (Francis et al., 2013). Moreover, the R-spondin receptor Lgr4 is essential for both prostate development as well as differentiation (Luo et al., 2013). We found that organoids express *Lgr4* and *Lgr5* (Figure S1I). DHT was not essential but significantly enhanced the efficiency of organoid formation (Figures S1G and S1H). EGF was essential for both establishment and passaging. TGF-β pathway inhibition was required for passaging of AP- and VP-derived organoids, but not for DLP-derived organoids (Figures S1F–S1H).

Both Luminal and Basal Cells Can Generate Murine Prostate Organoids

The availability of a robust in vitro murine prostate organoid system with basal and luminal layers allowed us to determine whether isolated basal or luminal cells are capable of establishing organoids. We separated basal and luminal cells from primary mouse prostate tissue using FACS. Basal cells were isolated based on high CD49f expression (also called α6-integrin) (Goldstein et al., 2008), luminal cells were captured based on expression of CD24 (also called heat stable antigen [HAS]; Figure 2A). CD24 was previously shown to specifically mark luminal cells in the human prostate (Liu et al., 2004), and CD24 expression has been used in conjunction with CD49f to isolate murine luminal cells (Lawson et al., 2007). We confirmed luminal-specific high CD24 expression in murine prostate tissue by IHC (Figure S2A). The purity of our sorted basal and luminal population was verified using qPCR for basal- and luminal-specific markers, *Ck5* and *Probasin* (*Pbsn*) (Figure 2B), and costaining for luminal-cell-specific Ck8 and basal-cell-specific Ck5 (Figure S2B).

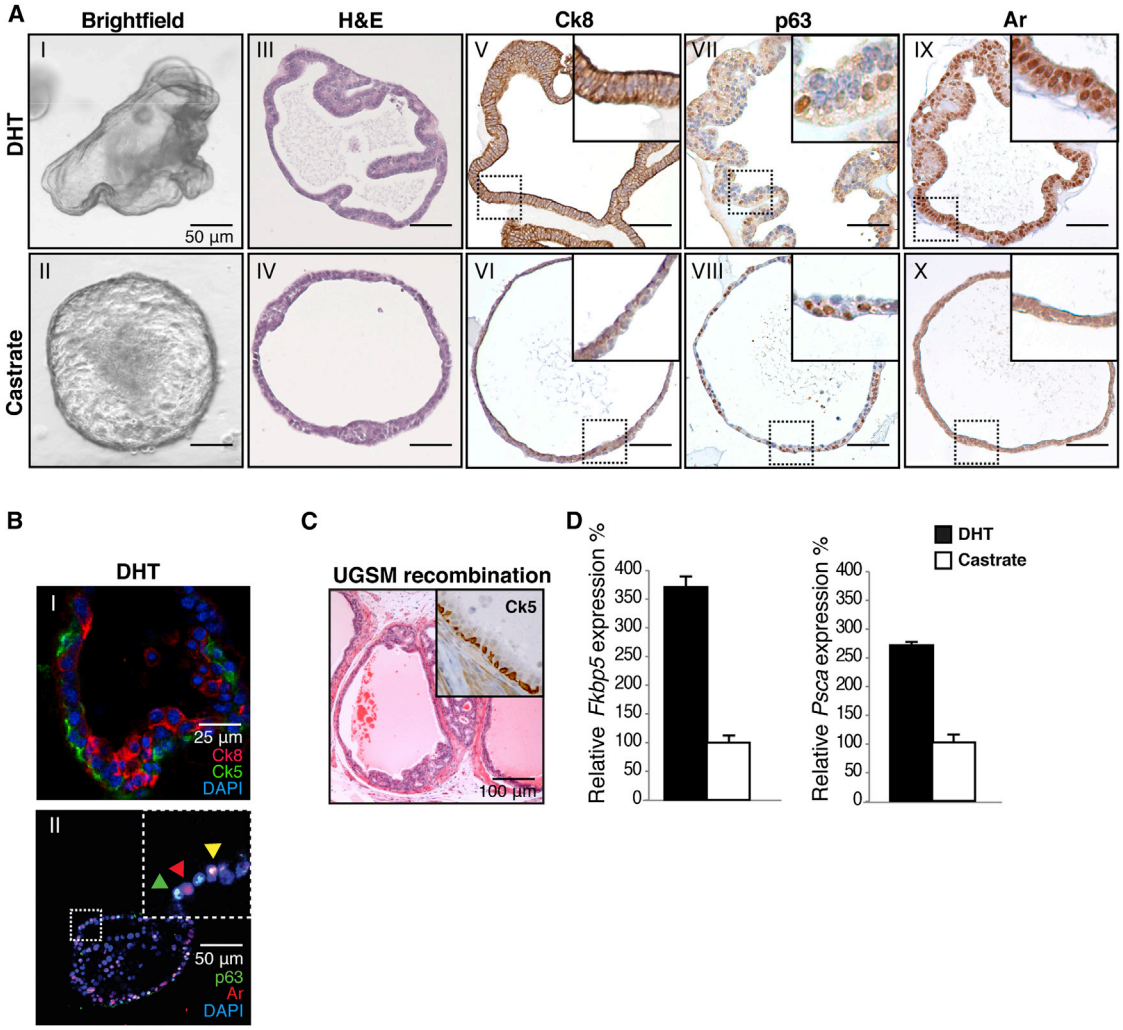

Figure 1. Establishment of Murine Prostate Cultures

(A) IHC analysis of murine organoids in the presence of DHT (1 nM) and in castrate conditions. Brightfield image (I and II) H&E staining (III and IV) Ck8 (V and VI) p63 (VII and VIII) Ar (IX and X). Strong increase in cell size is observed upon DHT addition as well as nuclear localization of the Ar. Scale bars, 50 μm.

(B) IF staining (I) of basal Ck5 (green) and luminal Ck8 (red) in organoids. Distinct luminal and basal cell populations are present in organoids. Bottom (II) staining for p63 (green) and Ar (red) showing single positive (green and red arrowhead) and double-positive Ar/p63 cells (yellow arrowhead).

(C) H&E stain of UGSM recombination 8 weeks after transplantation of 50,000 organoid cells derived from wild-type mice. Inset; Ck5 staining, confirming presence of basal cells.

(D) Quantitative RT-PCR of Ar targets *Psca* and *Fkbp5* in the presence of DHT (1 nM) and in castrate conditions (24 hr). *Psca* and *Fkbp5* transcripts are increased upon DHT addition. Expression was normalized to *Hprt*. Results are shown as mean ± SD.

See also Figure S1

We found a contamination of 0.04% of Ck5+ basal cells (~2 cells in 5,000 cells, determined in two independent samples) in the CD24+ fraction.

To measure their organoid-forming capability, we seeded 200 single basal- or luminal-derived cells in culture, i.e., one cell per Matrigel drop. Approximately 15% of basal cells formed an organoid, compared to 1% of luminal cells (Figure 2C). Yet, the growth of luminal cells could not be explained by the presence of contaminating basal cells. Considering 15% of basal cells grow out, a basal cell contamination of >6% is required to explain an outgrowth efficiency of 1% of luminal cells, whereas we only found ~0.04% of contaminating basal cells. Finally, CD24/CD49f double-negative cells, which represent nonepithelial cells, did not grow (Figure 2C).

Despite the difference in cloning efficiency, we did not observe morphological differences in organoid development from single cells. Both luminal and basal cells initially formed a solid ball and subsequently developed into a sphere within 10 to 14 days (Figure S2C). IHC analysis showed that the organoids derived from either basal or luminal cells expressed both basal (p63, Ck5) and luminal (Ck8) markers and express Ar (Figure 2D). Furthermore, both luminal- and basal-derived murine organoids could be passaged long-term. These data are consistent with recent lineage-tracing studies (Choi et al., 2012; Wang et al.,

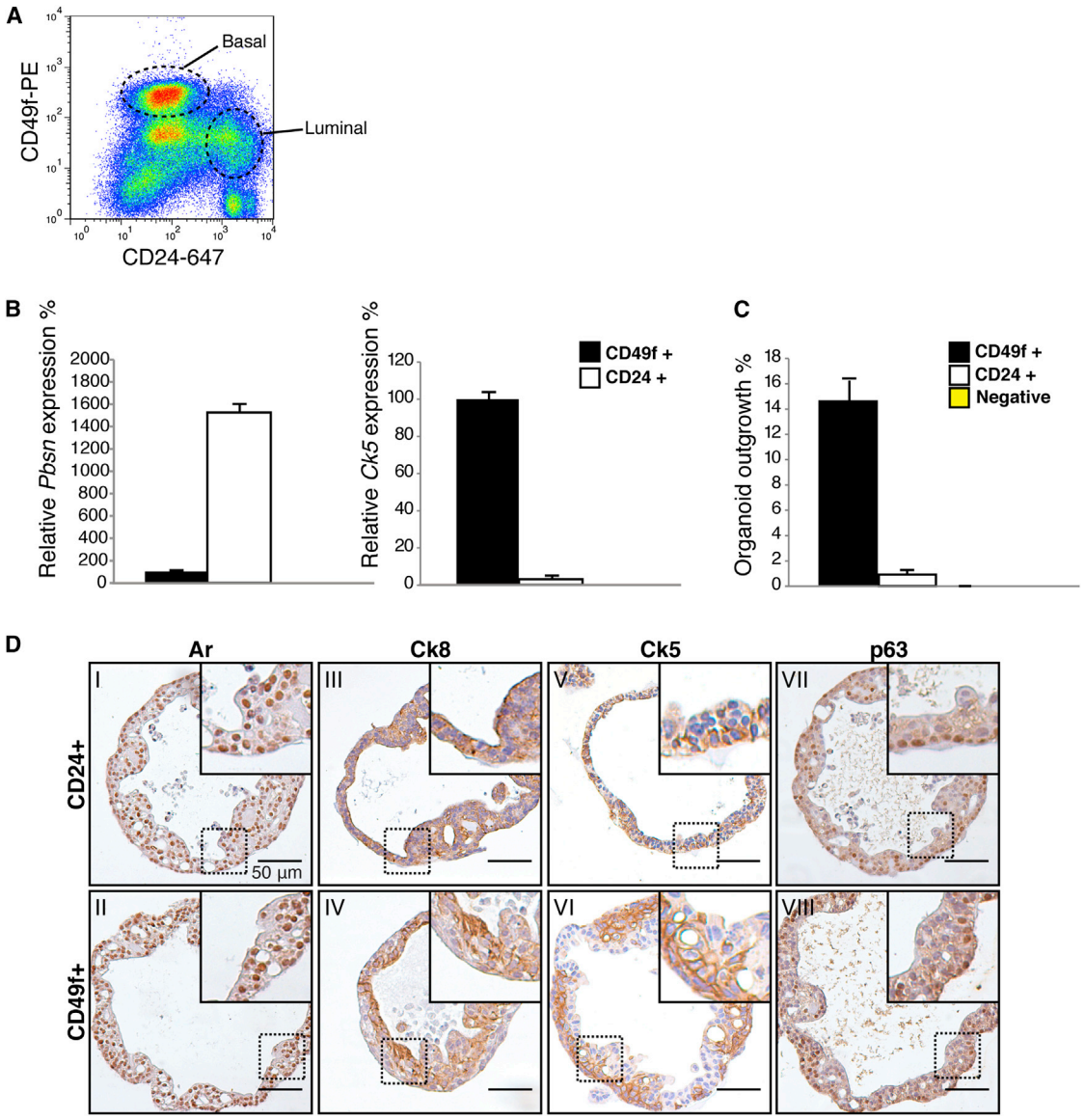

Figure 2. Basal and Luminal Cells Give Rise to Organoids

(A) FACS plot of CD24 (luminal) CD49f (basal) stained murine prostate.

(B) Quantitative RT-PCR expression analysis of basal (*Ck5*) and luminal (*Probasin, Pbsn*) marker expression in CD24+ luminal and CD49f+ basal cells. *Pbsn* is strongly expressed in luminal cells; *Ck5* is strongly expressed in basal cells. Expression was normalized to *Hprt*. Results are shown as mean ± SD.

(C) Percentage of organoids established by 200 single cells 14 days postseeding. Approximately 15% of basal cells generate an organoid. 1% of luminal cells generate an organoid. Results are shown as mean ± SD.

(D) IHC stainings of single-cell-derived murine prostate organoids, showing similar staining patterns of Ar (I and II), Ck8 (III and IV), Ck5 (V–VI) and p63 (VII and VIII) and morphology, showing that basal cells and luminal cells are both capable of giving rise to both epithelial lineages. Scale bars, 50 μm.

See also Figure S2

2009; Wang et al., 2013) and support the existence of prostate stem cells in both the basal and luminal compartments of the normal mouse prostate.

Murine Prostate Organoids as a Tool for Cancer Biology

To explore the suitability of prostate organoid cultures for genetic studies, we asked if we could generate cancer phenotypes using known prostate cancer oncogenes or tumor suppressor genes that have been previously characterized in genetically engineered mouse models (GEMMs). We established organoids from mice with a floxed Pten allele (*Pten*$^{loxP/loxP}$) (Di Cristofano et al., 1998), a *TMPRSS2:ERG* gene fusion (*Rosa26* $^{LSL-ERG}$) (Chen et al., 2013) or bigenic *Pten*/Rosa26$^{LSL-ERG}$ mice and compared their phenotypes to organoids derived from wild-type mice. In these experiments, Cre-driven excision of loxP-flanked regions was mediated by the prostate-specific

composite promoter ARR_2PB (PBCre) (Figure S3A). Cultures carrying the prostate-specific *Pten* deletion initially formed normal-appearing organoids containing a lumen, but within a week the organoids had multiple layers of epithelium, eventually forming a nearly solid 3D structure (Figure 3A). Histologically, PBCre $Pten^{loxP/loxP}$ organoid resembled phenotypes observed in vivo (Carver et al., 2011), with features reminiscent of high-grade PIN. Organoids derived from PBCre Rosa26 $^{LSL\text{-}ERG}$ mice showed no signs of neoplasia (Figures 3A and S3B), consistent with the in vivo phenotype (Carver et al., 2009; Chen et al., 2013). The combination of *Pten* deletion and ERG overexpression yielded a hyperplastic phenotype similar to that seen with *Pten* deletion alone (Figures 3A and S3B), but with "fingers" protruding into the Matrigel (Figure 3A), suggesting invasive behavior. All organoids responded to DHT withdrawal with reduced *Fkbp5* expression (Figure S3C). Furthermore, the histologic features attributable to *Pten* and ERG in vitro were confirmed in UGSM tissue recombination experiments of transplanted passage-8 organoids (Figure S3B).

To determine the suitability of prostate organoids for ex vivo genetic manipulation, we silenced *Pten* expression in PBCre $Rosa26^{LSL\text{-}ERG}$ organoids by infection with lentivirus encoding a shRNA targeting *Pten*. Puromycin selection was applied to ensure that only infected organoids remained (Figure 3B). Seven days postinfection, we observed an 80%–90% decrease in *Pten* mRNA levels (Figures 3C and S3D), accompanied by increased phosphorylation of AKT and ribosomal protein S6 (Figures 3D and S3E), consistent with increased PI3K activation. Remarkably, the sh*Pten*-infected organoids displayed hyperplastic phenotypes (Figure 3E). Similarly, sh*Pten*-infected Rosa26 $^{LSL\text{-}ERG}$ organoids generated hyperplastic prostate glandular tissue in UGSM tissue recombination experiments, similar to that seen in the $Pten^{loxP/loxP}$/$Rosa26^{LSL\text{-}ERG}$ grafts, control shRNA-infected organoids showed no signs of hyperplasia (Figure 3E). Similar to earlier work in GEMM models showing that hyperactive PI3K signaling in Pten null prostate tissue results in reduced Ar transcriptional activity due to negative feedback on Her kinase signaling(Carver et al., 2011), we observed reduced expression of the Ar target genes *Psca* and *Fkbp5* in organoids with *Pten* knockdown (Figures 3C and S3D). Collectively, these results show that in vitro prostate organoid phenotypes mimic in vivo phenotypes and that retroviral gene expression or gene knockdown in organoids can be used to identify and study genes involved in prostate cancer.

Establishment of Human Prostate Organoids with Basal and Luminal Cells

Based on our previous experience (Sato et al., 2011), we anticipated that human prostate organoid cultures might require additional growth factors. Fibroblast growth factor-10 (FGF10), FGF2, and prostaglandin E2 (PGE2) have been shown to support proliferation of prostate cell lines and/or human colon epithelium (Jung et al, 2011; Memarzadeh et al., 2007). Therefore, we added these to the "mouse" medium (ENR+A83-01+DHT). We also included nicotinamide and the p38 inhibitor SB202190, which have been previously identified as being essential for human small intestinal cultures (Sato et al., 2011). This combination of growth factors enabled us to establish and propagate human prostate epithelial organoids from 40 independent normal prostate specimens from patients undergoing radical prostatectomy. Human prostate organoids have been passaged for >12 months with no obvious phenotypic changes over time and with stable, normal karyotypes (Figures S4A and S4B). To determine the genetic stability of our organoid cultures at the nucleotide level, we performed whole-exome sequencing on passage 2 and passage 7 organoids. To detect genetic changes that developed during in vitro expansion, we filtered single-nucleotide variants (SNVs) and small insertions and deletions (indels) observed in the long-term culture for presence in the short-term culture (see Experimental Procedures). Subsequently, candidate changes that emerged using this approach were independently examined (Table S1). In addition, we also checked for cases of loss of heterozygosity in the passage 7 cultures compared to passage 2 cultures. We did not observe any genetic variants in the passage 7 culture that were not present in the passage 2 culture, implying that the organoid cultures remain genetically stable over time.

Initially, we observed solid spherical structures with multiple layers of epithelium, which progressed over 2–3 weeks to organoids with easily visible lumens. Areas of single-layered as well as double-layered epithelium were observed. The majority of cells were positive for the luminal epithelial markers CK8 and AR (Figures 4A–4C). Typically, cells expressed either the basal marker CK5 or the luminal marker CK8. Cells positive for basal markers p63 and CK5 were also present and were always located in the outer layer of organoids (Figures 4A–4C). Similar to mouse-derived prostate organoids, human organoids expressed prostate-specific genes such as *PSA* (Figures 4D–4E) and *NKX3.1* (Figurse 4B and 4E). Additionally, human organoids retained intact AR signaling as measured by dose-dependent induction of *PSA* mRNA by DHT (Figure 4D) and reduced expression of *NKX3.1* and *PSA* upon DHT withdrawal (Figure 4E). In addition, human organoids formed prostate glands in UGSM tissue recombination assays when transplanted after 8 passages (Figure 4F), as also seen with murine prostate organoids.

Having established conditions for human prostate organoid cultures, we examined the relative requirement for each growth factor in maintaining the cultures. EGF, FGF2, nicotinamide, PGE2 and the TGF-β pathway inhibitor A83-01 were all essential to sustain prolonged organoid growth (Figures S4C and S4D). Removal of the p38 kinase inhibitor SB202190 did not lead to a decrease in organoid formation capacity but did result in histologic evidence of keratinization, perhaps due to increased stress signaling. Although passaging was not affected by the removal of FGF10, Noggin or R-spondin, the efficiency of organoid formation upon initial plating was reduced. Moreover, removal of any one of these factors, as well as of nicotinamide, resulted in decreased AR expression levels. In particular, removal of R-spondin or Noggin led to a virtual disappearance of AR expression (Figures 4G and S4E). Withdrawal of EGF resulted in a modest upregulation of AR mRNA and protein level together with a potent increase in expression of the AR target gene *PSA* (Figures S4F–S4H). These data are consistent with a negative feedback loop involving EGF and AR signaling and/or an inhibitory effect of high levels of EGF signaling on the generation or survival of luminal cells.

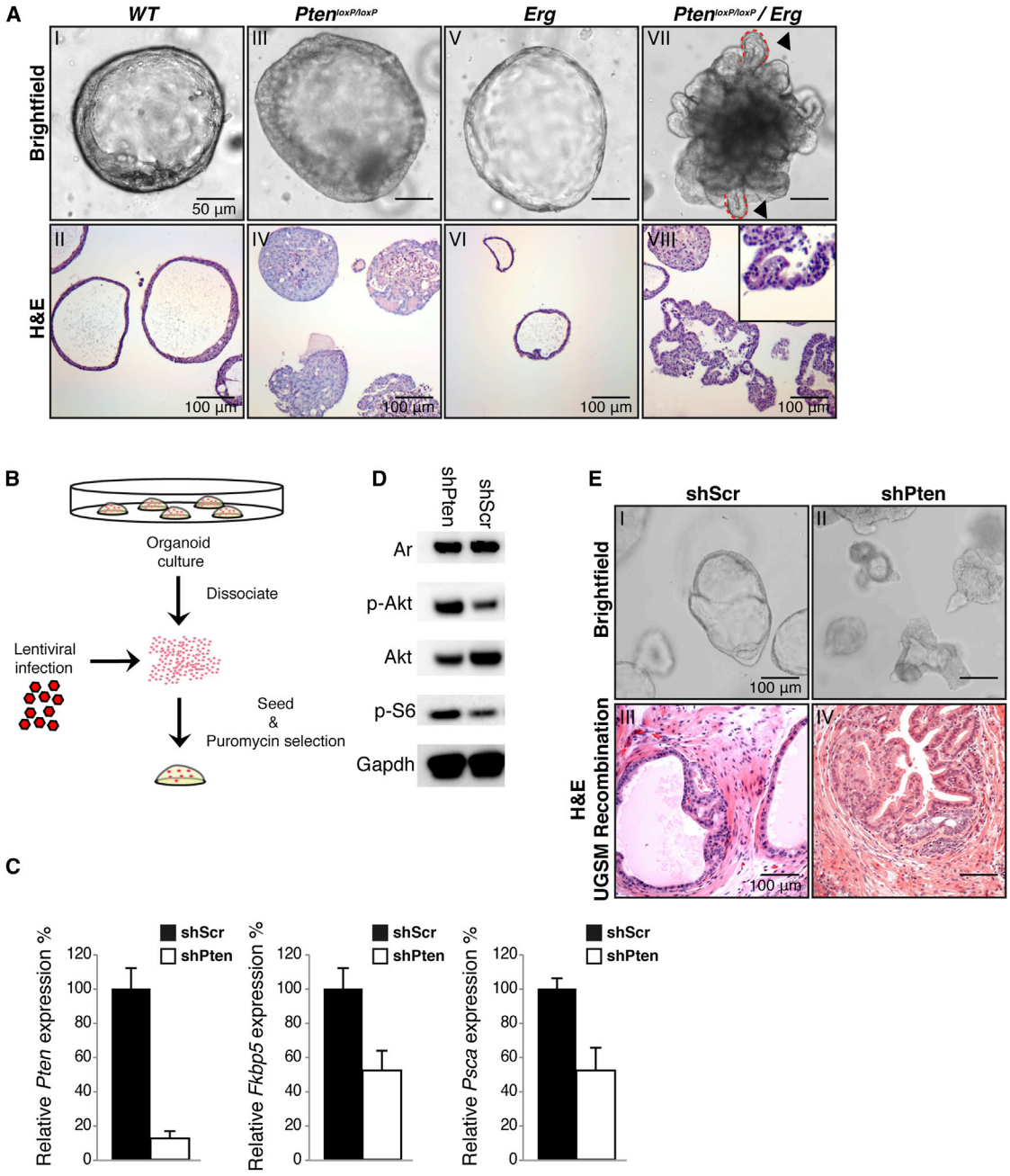

Figure 3. Genetically Engineered Mouse Prostate Cancer Models Are Recapitulated in Organoids

(A) Brightfield and H&E images of wild-type (WT) (I and II), PBCre Pten$^{loxP/loxP}$ (III and IV), PBCre Rosa$^{LSL-ERG}$ (V and VI), and PBCre Pten$^{loxP/loxP}$ Rosa$^{LSL-ERG}$ (VII and VIII). In Pten$^{loxP/loxP}$ organoids the lumen is filled with hyperplastic cells. Pten$^{loxP/loxP}$/Rosa26$^{LSL-ERG}$ organoids make fingerlike protrusions are made into the Matrigel (arrowheads, dashed lines, inset VIII).

(B) Schematic overview of retroviral infection.

(C) Quantitative RT-PCR analysis of *Pten, Fkbp5*, and *Psca* expression in shPten- and shScr-control-infected PBCre Rosa26 $^{LSL-ERG}$ organoids. Upon *Pten* knockdown, Ar target gene expression is diminished. Expression was normalized to *Hprt*. Results are shown as mean ± SD.

(D) Western blot analysis of PI3K pathway activation in shPten- and ShScr-control-infected PBCre Rosa26 $^{LSL-ERG}$ organoids. p-Akt and p-S6 levels are increased upon *Pten* knockdown.

(E) Brightfield image of shPten-RFP shScr-RFP-infected PBCre Rosa26$^{LSL-ERG}$ organoids (I and II) and corresponding H&E staining of shPten/shScr organoid-UGSM recombinations (III and IV) showing hyperplastic phenotype in organoids and in UGSM recombinations upon *Pten* knockdown.

Scale bars in (A), (B), and (E) represent 50 µm unless noted differently. See also Figure S3

Human Prostatic Epithelium Harbors Both Luminal and Basal Stem Cells

Existing human prostate culture methods favor outgrowth of basal epithelial cells that, in UGSM tissue recombination assays, can generate prostate tissue with luminal cells, providing evidence for human prostate stem cells in the basal epithelium (Garraway et al., 2010; Goldstein et al., 2008). However, experimental evidence for the existence of a human luminal stem cell is lacking. Our success in propagating human organoids with basal and luminal cells provided a unique opportunity to address this question.

As with our mouse studies, we separated basal and luminal cells from human prostate tissue by FACS. Basal cells were isolated on the basis of high CD49f expression, and luminal cells by the cell surface marker CD26 (also called DPPIV) (Liu et al., 2004) (Figure 5A). Staining of these two populations for CK5 and CK8 postisolation verified their basal and luminal cellular identities (Figure S5A). Additionally, we stained for the luminal marker NKX3.1 and found that essentially all CD26-sorted cells express NKX3.1 (Figure S5B). Although CD26 and CD49f are also expressed on immune cells, we only found very low numbers of contaminating hematopoietic cells as measured by the panleukocyte marker CD45 (<0.1% in 10,000 cells, three independent samples). We detected very little contamination of CK5+ basal cells (<0.2%, 18 ± 1.7 in 10,000 cells, three independent samples) in the FACS-purified luminal population.

To determine their relative organoid-forming ability, we seeded single basal or luminal cells at varying densities. Human basal cells were highly efficient at establishing organoids, be it at single-cell density (70%) or at high density (1,000 cells/10 μl) (Figure 5B). Luminal cells also established organoids, albeit at much lower efficiency (1%–2%), both at single cell and at high density seeding. Of note, this could not be explained by contaminating basal cells, as these were present at a >10-fold lower frequency (<0.2%), suggesting the presence of a rare luminal organoid-forming cell.

Within 7 days of plating, single basal cells formed solid spheres that, within 2–3 weeks, contained lumens resembling organoids grown from bulk tissue, when viewed by brightfield microscopy. However, unlike bulk-derived organoids, IHC analysis revealed that the majority of cells in basal-derived organoids expressed CK5, with CK8 cells surrounding a sporadic array of lumens within a single organoid (Figure 5C). AR expression was patchy, but tended to be near lumens (Figure 5C, Figure S5C). In contrast to basal-cell-derived organoids, those generated from luminal cells immediately formed lumens and thus could be easily distinguished from basal-derived organoids by brightfield. IHC analysis of luminal-derived organoids revealed a majority of cells expressing CK8 and AR, consistent with a true luminal phenotype. Strikingly, CK5-positive, CK8-negative cells were also observed (Figure 5C), indicating that human luminal cells can generate basal cells. Consistent with their differing histology, the luminal markers *NKX3.1* and *PSA* were strongly expressed in luminal organoids whereas the basal marker *p63* was more highly expressed in basal organoids (Figure 5D, 5E). Both organoid types retained AR pathway signaling, as DHT withdrawal led to a significant decrease in *PSA* expression levels (Figure 5E) and a reduced nuclear localization of AR (Figure S5H).

Both basal- and luminal-derived organoids could be passaged for at least 4 months and maintained a stable karyotype (Figure S5D). A more detailed analysis of relative growth factor requirements revealed few differences compared to bulk human organoid cultures (Figures S5E and S5F), most notably that luminal organoids were more dependent on R-spondin for serial passaging. Expression analysis using RT-PCR of Lgr receptors revealed that *LGR4* is expressed in both types of human organoids (Figure S5G). The relative dependence of luminal cells on R-spondin/Lgr signaling is also suggested by the reported failure of luminal differentiation by $Lgr4^{-/-}$ prostate progenitor cells (Luo et al., 2013). DHT drastically enhanced luminal organoid formation but, as observed with mouse, was not absolutely required for organoid maintenance (Figures S5E and S5F). The p38 inhibitor was not required to prevent keratinization. As seen with organoids derived from bulk tissue, we observed a loss of nuclear AR staining as well as a decrease in AR protein levels upon DHT withdrawal (Figure S5H). We also observed a strong increase in *PSA* expression upon EGF withdrawal in both luminal- and basal-cell-derived organoids (Figure S5I).

To formally demonstrate that single luminal cells can give rise to organoids containing both lineages, we repeated these experiments after plating single luminal cells. As observed in bulk, single basal-cell-derived organoids proliferated much faster over time than single luminal-cell-derived organoids. As observed in bulk, luminal cells quickly formed lumens, whereas basal cells first formed solid spheres (Figure 6A). IF staining of single cell-derived organoids showed that both basal and luminal cells generated organoids containing both lineages as demonstrated by the presence of CK8+ luminal and CK5+ basal cells (Figure 6B), providing conclusive evidence for a human multiprogenitor prostate cell in the luminal compartment.

DISCUSSION

Leveraging our previous experience establishing organoid cultures, we have devised a culture system that allows long-term expansion of murine and human prostatic epithelium. The resulting organoids retain both basal and luminal epithelial layers and preserve androgen-responsiveness in culture. Organoids differ significantly from earlier descriptions of prostate spheres, which consist primarily of CK5+ basal cells with luminal-like features in response to DHT treatment, but lack NKX3.1+ cells or secretions (Xin et al., 2007). In contrast, our culture conditions induce full luminal differentiation. These conditions were developed using growth factors originally optimized for intestinal epithelia, with some modifications. We conducted studies to address the requirement for each of these growth factors when removed from the complete cocktail, but have not exhaustively examined all possible perturbations.

Organoids proliferate at a much higher rate compared to normal prostate. We assume that organoid culture conditions mimic a regenerative response. In contrast to gastrointestinal organoid cultures, R-spondin is not essential for maintenance of prostate organoid cultures. However, organoid establishment and growth is enhanced by R-spondin. Importantly, expression of AR is strongly dependent on R-spondin. Taken together, our data and previous studies suggest that R-spondin/Lgr

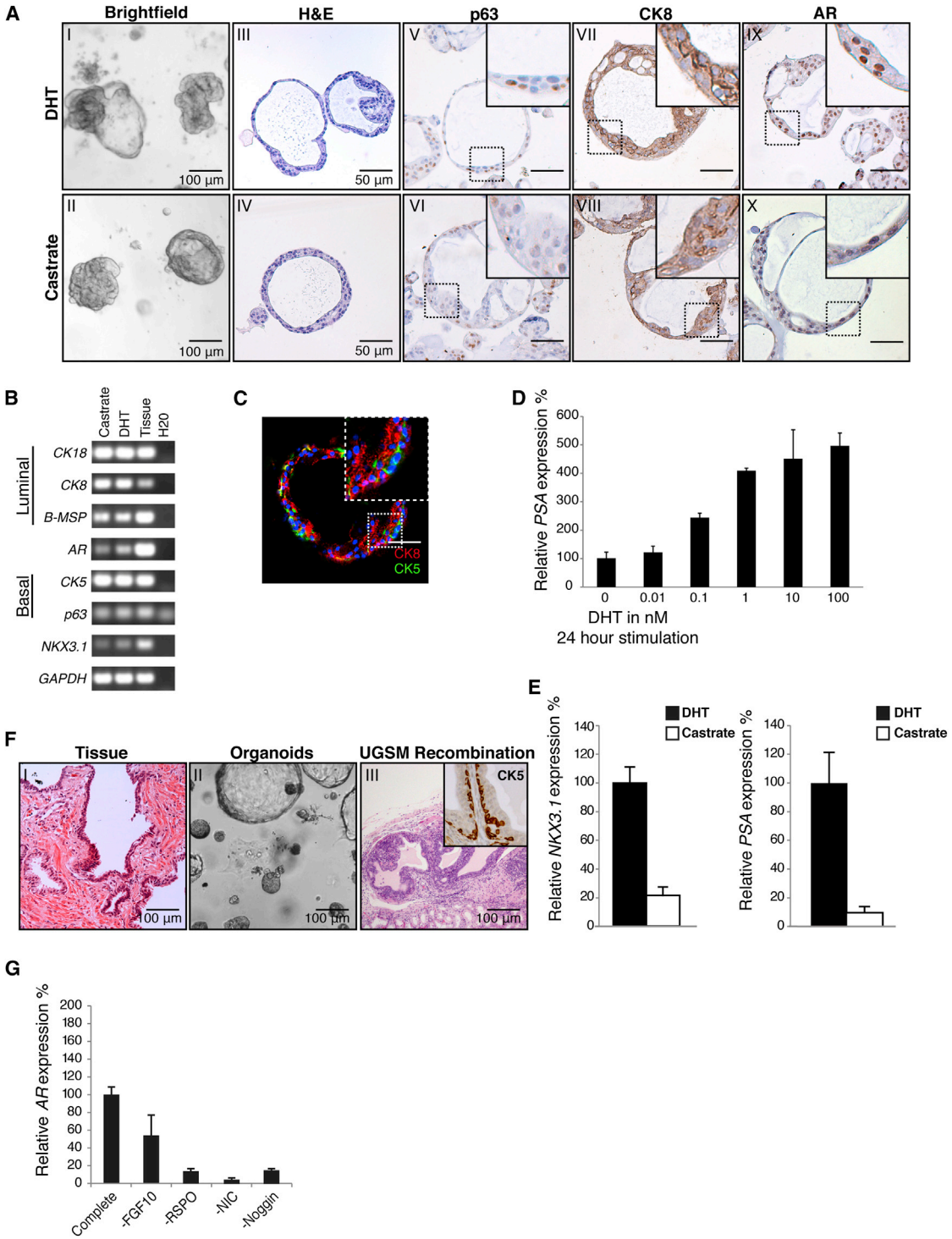

Figure 4. Establishment of Human Prostate Organoid Cultures

(A) IHC analysis of passage 6 (12 week) human organoids in the presence of DHT (1 nM) and in castrate conditions. Brightfield image (I and II), H&E staining (III and IV), p63 (V and VI), CK8 (VII and VIII), and AR (IX and X). Upon DHT addition nuclear localization of the AR is observed. Scale bars, 50 µm unless noted differently.

(B) RT-PCR analysis of prostate organoids show that both luminal and basal markers are expressed in the absence and presence of DHT (1 nM).

(C) IF staining of basal CK5 (green) and luminal CK8 (red) in organoids. Distinct luminal and basal cell populations are present in organoids.

(D) Quantitative RT-PCR analysis of *PSA* 24 hr after DHT stimulation (0–100 nM). Expression was normalized to *GAPDH*. Results are shown as mean ± SD (n = 3)

(E) Quantitative RT-PCR analysis of AR targets *NKX3.1* and *PSA* in the presence of DHT (1 nM) and without DHT (castrate) (24 hr). Upon DHT addition, a strong increase of *PSA* and *NKX3.1* transcript is observed. Expression was normalized to *GAPDH*. Results are shown as mean ± SD (n = 3).

(legend continued on next page)

signaling is important for luminal cell differentiation and luminal cell maintenance.

Several other factors, like FGF10 and Noggin, favor differentiation toward a luminal phenotype, by positively regulating AR expression. It is plausible that, in vivo, the stroma supplies most if not all of these factors. Work from others has demonstrated that the Rho/ROCK kinase inhibitor Y-27632 allows long-term culture of primary epithelial tissue cultures, including prostate, in conjunction with stroma-derived feeder cells (Liu et al., 2012). Possibly, the growth factor composition of our culture method mimics the factors secreted by the feeder cells in this method. In contrast to our method, AR responsiveness is not well defined in this system. Preliminary studies of Y-27632 in our system suggest a benefit in initiating single cell organoid cultures, but not in propagation of established organoids.

The availability of a robust culture model that generates prostate organoids containing both basal and luminal cells allowed us to address the important question of whether basal or luminal cells (or both) are required to generate a complete prostate organoid. Prior efforts to explore the ''prostate stem cell'' question have primarily relied on UGSM tissue recombination assays. These experiments have shown that tissue-regenerating activity primarily resides in basal cell populations (Goldstein et al., 2008). However, murine lineage-tracing studies demonstrate that both basal and luminal cells are self-renewing, including evidence that luminal cells can give rise to basal cells (Choi et al., 2012; Wang et al., 2013). Our culture method confirms that basal and luminal cells can each generate a complete multilayer prostate organoid and shows repopulating potential of human prostate luminal cells which can generate both basal and luminal lineages. Although these luminal progenitor cells occur at lower frequency than their basal counterparts, they give rise to more normal appearing organoids and therefore could have greater physiologic relevance. Their frequency (~1% of all luminal cells) raises the question of whether these CD26+ and NKX3.1+ luminal cells may be the human equivalent of the murine castration-resistant Nkx3.1+ cell (CARN) (Wang et al., 2009).

This culture method, compared to other experimental procedures, uniquely allows for elucidation of the cellular identity of this human luminal progenitor. In the absence of evidence of neuroendocrine differentiation, we refer to these luminal and basal cells as multipotent progenitors rather than stem cells. Modifications to the culture conditions may reveal that these cells may also have neuroendocrine cell repopulating potential.

In addition to their utility in defining prostate epithelial lineage relationships, the organoid model has the potential to greatly facilitate functional genetic studies, particularly in cancer genomics. Several large-scale prostate cancer genome resequencing studies have now defined a plethora of novel genomic alterations in primary and metastatic cancer whose functions are currently unknown (Barbieri et al., 2012; Grasso et al., 2012; Taylor et al., 2010). Here, we have shown that murine prostate organoids faithfully recapitulate in vivo phenotypes known from prostate cancer GEMMs. Moreover, the organoids are easily manipulated with inhibitors, retroviruses and CRISPR/Cas9 (Schwank et al., 2013), offering a tool to study the impact of these manipulations on growth, invasive behavior, and drug sensitivity. Organoid culture may also represent a straightforward, cheap, and robust alternative to xenografting.

There is considerable interest in whether these same culture conditions can be used to generate organoids from human prostate cancers. If successful, this technology could help address a huge need in the prostate cancer biology field for a broad array of human prostate cancer cell lines, which has been forced to rely on the very few such cell lines that have been established to date. In a companion paper, Gao et al. (2014, this issue) show that this culture method does allow efficient and sustained growth of human prostate cancer organoids isolated from men with advanced disease that faithfully retain the genomic characteristics of the originating human tissue sample. We have conducted similar studies using primary human prostate cancer samples but failed to establish renewable primary cancer organoid lines, due to overgrowth by normal prostate epithelial cells present within each tumor sample. The notion that cells harboring oncogenic mutations grow slower than normal cells may be counterintuitive, yet we also observe this consistently for colorectal and pancreas cancers. The observed increased rates of apoptosis in cancer organoid cultures may reflect the high levels of genomic instability. The absence of normal prostate cells in metastatic samples may explain the high rate of success of our method in that context. Efforts to overcome this complication by purification of tumor cells from normal epithelium are ongoing. Taken together, prostate organoid technology offers a platform for mechanistic studies of prostate development, homeostasis, and cancer.

EXPERIMENTAL PROCEDURES

Isolation and Culture of Prostate Epithelial Cells

Murine prostates were divided into three lobe pairs; AP, DLP, and VP. Lobes were enzymatically digested with collagenase type II (GIBCO) and subsequently with TrypLE (GIBCO). Cells were seeded in growth factor reduced Matrigel (Corning) and overlayed with medium containing the growth factors: EGF 5-50 ng/ml (Peprotech), R-spondin1 conditioned medium or 500 ng/ml recombinant R-spondin1 (Peprotech), Noggin conditioned medium or 100 ng/ml recombinant Noggin (Peprotech), and the TGF-β/Alk inhibitor A83-01 200 nM (Tocris). Dihydrotestosterone (DHT) (Sigma) was added at 0.1–1 nM. Human prostate samples were obtained from patients undergoing radical prostatectomy according to guidelines from the UMC Utrecht. Prostate tissue was enzymatically digested with collagenase type II and subsequently with TrypLE. Cells were seeded in growth factor reduced Matrigel and cultured in medium containing growth factors as above, with the addition of 10 ng/ml FGF10 (Peprotech), 5 ng/ml FGF2 (Peprotech), 1 μM Prostaglandin E_2 (Tocris), 10 μM SB202190 (Sigma-Aldrich), 10 mM nicotinamide (Sigma-Aldrich), and DHT 0.1–1 nM. For detailed summary of culture medium composition see Extended Experimental Procedures.

(F) H&E stain of UGSM recombination 8 weeks after transplantation of 50,000 human organoid cells derived. Inset; CK5 staining, confirming presence of basal cells. Scale bars, 100 μm.

(G) Quantitative RT-PCR of *AR* mRNA levels in the absence of growth factors. Withdrawal of Noggin, R-spondin, FGF10, and nicotinamide led to reduced *AR* expression. Expression was normalized to *GAPDH*. Results are shown as mean ± SD.

See also Figure S4.

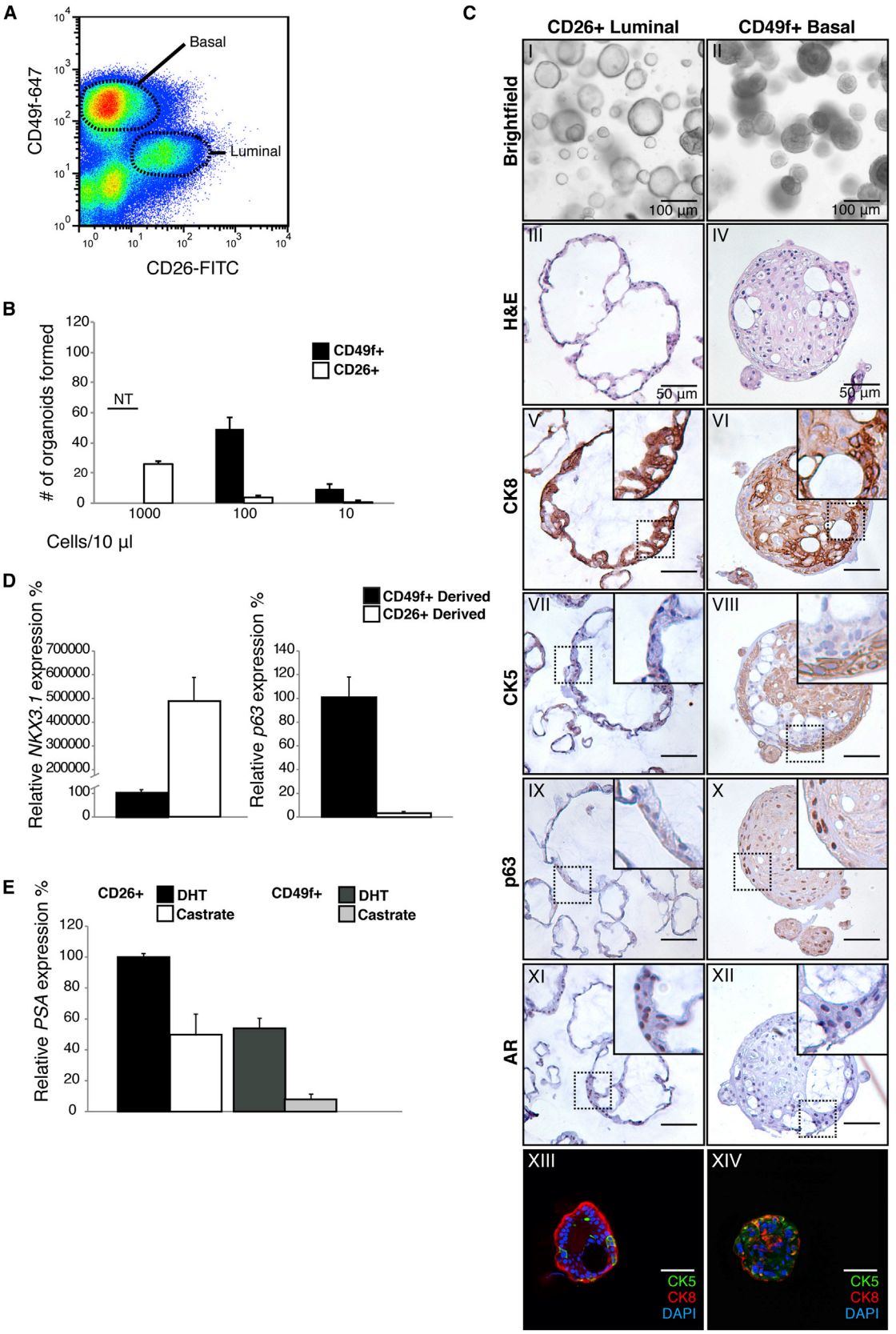

(legend on next page)

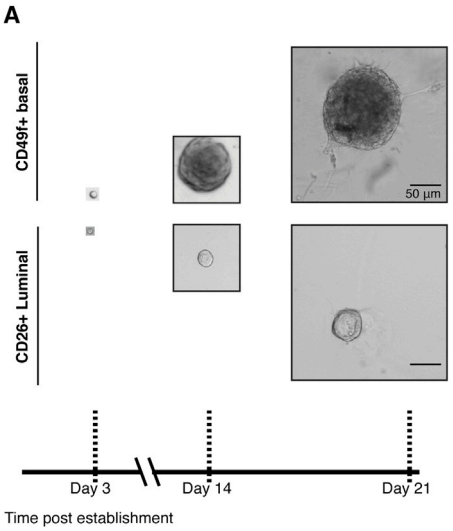

Figure 6. Single Human Basal and Luminal Cells Give Rise to Organoids

(A) Brightfield images of organoids grown from single CD26+ luminal and CD49f+ basal cells.

(B) IF stain of CK5 (green) and CK8 (red) showing distinct basal and luminal cells in single luminal-cell- and single basal-cell-derived organoids (passage 4). Scale bars, 50 μm.

FACS

Single cell suspensions of human cells were stained using CD49f-alexa 647 (1:200, GoH3, BD Biosciences) and CD26-FITC (1:200, M-A261, eBioscience). Murine cells were stained using a CD49f-PE (1:200, GoH3, BD Biosciences) and CD24-alexa 647 (1:200, 30-F1, eBioscience).

UGSM Essay

UGSM recombination essay was performed as described previously (Xin et al., 2003). All mouse work was performed in accordance with national guidelines and regulations of the Hubrecht institute (DEC committee) or Memorial Sloan Kettering Cancer Center (RARC committee).

Genetic Analysis

DNA was isolated from early (P2) and late (P7) passage organoids. Whole-exome sequencing and genetic analysis were done as described previously (DePristo et al., 2011; Li and Durbin, 2009). Detailed discription is given in Extended Experimental Procedures. The data for the whole-exome sequencing were deposited to the EMBL European Nucleotide Archive, accession number: ERP006541.

Immunohistochemistry and Immunofluorescence

Organoids were processed and stained as described previously(Sato et al., 2009). The following antibodies were used for staining on murine and human prostate organoids AR (1:1,000, N-20, Santa Cruz), CK5 (1:2,000, AF-138, Covance), CK8 (1:50, C-51, Santa Cruz), p63 (1:800, 4A4, Millipore). Stainings were visualized with bright vision (Dako). For IF organoids were stained for AR (1:200) Ck5 (1:500), Ck8 (1:50), p63 (1:500) using the antibodies described above and NKX3.1 (rabbit, 1:100, kind gift of Michael Shen). Secondary antibodies were conjugated with Alexa-Fluor (−488, −568, −647). DNA was stained with DAPI.

Lentiviral Infections

Lentiviral infections were performed as described previously (Koo et al., 2012) using pLKO.1-puro-UbC-TagFP635 (Sigma) targeting *Pten* (CGACT TAGACTTGACCTATAT) or control Scramble (CC TAAGGTTAAGTCGCCCTCG).

Western Blot

Membranes were probed with antibodies directed against AR (1:1,000, N-20, Santa Cruz), GAPDH (1:2,000 Abcam) AKT (1:1,000 Cell Signaling #9272), phosphorylated-AKT (Ser473) (1:1,000 Cell Signaling #4060), and phosphorylated-S6 (Ser235/Ser236) (1:1,000, Cell Signaling #2211). Signal was visualized with secondary HRP conjugated antibodies and ECL.

ACCESSION NUMBERS

The EMBL European Nucleotide Archive accession number for the whole-exome sequencing reported in this paper is ERP006541.

SUPPLEMENTAL INFORMATION

Supplemental Information includes Extended Experimental Procedures, five figures, and three tables and can be found with this article online at http://dx.doi.org/10.1016/j.cell.2014.08.017.

AUTHOR CONTRIBUTIONS

W.R.K. and H.C.C. conceived and oversaw project. W.R.K. and P.J.I. performed isolation of mouse organoids. P.J.I. and J.W. performed xenograft experiments. W.R.K., J.D., A.G. performed human organoid experiments. C.M.D. and D.G. provided assistance with cell-isolation and xenografts. W.R.K. and H.B. performed IHC/IF. N.S. and R.G.J.V. gave essential input. Y.C. provided GEMM models. W.R.K., J.D., C.L.S., and H.C.C. wrote manuscript. R.v.B. and E.C. performed sequencing experiments.

ACKNOWLEDGMENTS

R.v.B. and E.C. were supported by the Netherlands Genomics Initiative Zenith grant (935.12.003). J.D. was supported by NWO-ZonMw VENI (91614138). N.S. was supported by EU/232814-StemCellMark. C.L.S. and Y.C. were

Figure 5. Establishment of Human Prostate Organoid Cultures from Luminal and Basal Cells

(A) FACS plot of human prostate cells stained with CD26 (luminal) and CD49f (basal) markers.

(B) Organoid outgrowth from CD49f+ basal and CD26+ luminal cells at varying densities. Results are shown as mean ± SD. *NT, nontestable. At higher densities CD49f-derived organoids fuse, making counting of organoid number therefore unreliable. Results are shown as mean ± SD.

(C) Analysis of CD26-derived (luminal) and CD49f-derived (basal) organoids at passage 4. Brightfield picture (I and II) H&E staining (III and IV) CK8 (V and VI) CK5 (VII and VIII) p63 (IX and X) AR (XI and XII) IF stain of CK5 (green) and CK8 (red) showing distinct basal and luminal cells (XIII and XIV). Scale bars, 50 μm unless noted otherwise.

(D) Quantitative RT-PCR expression analysis of the luminal marker *NKX3.1* and basal marker *p63* in luminal and basal organoids at passage 4. Expression was normalized to *GAPDH*. Results are shown as mean ± SD.

(E) Quantitative RT-PCR of the AR target *PSA* in the presence of DHT (1 nM) and in castrate conditions (24 hr). Increased *PSA* mRNA levels are observed in both luminal- and basal-derived organoids after DHT treatment. Expression was normalized to *GAPDH*. Results are shown as mean ± SD.

See also Figure S5

supported by the PCF. W.R.K. and H.C.C. were supported by a Sta Op Tegen Kanker International Translational Cancer Research Grant. Stand Up To Cancer is a program of the Entertainment Industry Foundation administered by the American Association for Cancer Research. H.C.C. and W.R.K. are inventors of several patents related to organoid culture.

Received: April 10, 2014
Revised: July 8, 2014
Accepted: August 18, 2014
Published: September 4, 2014

REFERENCES

Barbieri, C.E., Baca, S.C., Lawrence, M.S., Demichelis, F., Blattner, M., Theurillat, J.-P., White, T.A., Stojanov, P., Van Allen, E., Stransky, N., et al. (2012). Exome sequencing identifies recurrent SPOP, FOXA1 and MED12 mutations in prostate cancer. Nat. Genet. *44*, 685–689.

Barker, N., Huch, M., Kujala, P., van de Wetering, M., Snippert, H.J., van Es, J.H., Sato, T., Stange, D.E., Begthel, H., van den Born, M., et al. (2010). Lgr5(+ve) stem cells drive self-renewal in the stomach and build long-lived gastric units in vitro. Cell Stem Cell *6*, 25–36.

Bhatia-Gaur, R., Donjacour, A.A., Sciavolino, P.J., Kim, M., Desai, N., Young, P., Norton, C.R., Gridley, T., Cardiff, R.D., Cunha, G.R., et al. (1999). Roles for Nkx3.1 in prostate development and cancer. Genes Dev. *13*, 966–977.

Binnerts, M.E., Kim, K.-A., Bright, J.M., Patel, S.M., Tran, K., Zhou, M., Leung, J.M., Liu, Y., Lomas, W.E., 3rd, Dixon, M., et al. (2007). R-Spondin1 regulates Wnt signaling by inhibiting internalization of LRP6. Proc. Natl. Acad. Sci. USA *104*, 14700–14705.

Carmon, K.S., Gong, X., Lin, Q., Thomas, A., and Liu, Q. (2011). R-spondins function as ligands of the orphan receptors LGR4 and LGR5 to regulate Wnt/beta-catenin signaling. Proc. Natl. Acad. Sci. USA *108*, 11452–11457.

Carver, B.S., Tran, J., Gopalan, A., Chen, Z., Shaikh, S., Carracedo, A., Alimonti, A., Nardella, C., Varmeh, S., Scardino, P.T., et al. (2009). Aberrant ERG expression cooperates with loss of PTEN to promote cancer progression in the prostate. Nat. Genet. *41*, 619–624.

Carver, B.S., Chapinski, C., Wongvipat, J., Hieronymus, H., Chen, Y., Chandarlapaty, S., Arora, V.K., Le, C., Koutcher, J., Scher, H., et al. (2011). Reciprocal feedback regulation of PI3K and androgen receptor signaling in PTEN-deficient prostate cancer. Cancer Cell *19*, 575–586.

Chen, Y., Chi, P., Rockowitz, S., Iaquinta, P.J., Shamu, T., Shukla, S., Gao, D., Sirota, I., Carver, B.S., Wongvipat, J., et al. (2013). ETS factors reprogram the androgen receptor cistrome and prime prostate tumorigenesis in response to PTEN loss. Nat. Med. *19*, 1023–1029.

Choi, N., Zhang, B., Zhang, L., Ittmann, M., and Xin, L. (2012). Adult murine prostate basal and luminal cells are self-sustained lineages that can both serve as targets for prostate cancer initiation. Cancer Cell *21*, 253–265.

Cook, C., Vezina, C.M., Allgeier, S.H., Shaw, A., Yu, M., Peterson, R.E., and Bushman, W. (2007). Noggin is required for normal lobe patterning and ductal budding in the mouse prostate. Dev. Biol. *312*, 217–230.

Cunha, G.R. (1973). The role of androgens in the epithelio-mesenchymal interactions involved in prostatic morphogenesis in embryonic mice. Anat. Rec. *175*, 87–96.

de Lau, W., Barker, N., Low, T.Y., Koo, B.-K., Li, V.S., Teunissen, H., Kujala, P., Haegebarth, A., Peters, P.J., van de Wetering, M., et al. (2011). Lgr5 homologues associate with Wnt receptors and mediate R-spondin signalling. Nature *476*, 293–297.

DePristo, M.A., Banks, E., Poplin, R., Garimella, K.V., Maguire, J.R., Hartl, C., Philippakis, A.A., del Angel, G., Rivas, M.A., Hanna, M., et al. (2011). A framework for variation discovery and genotyping using next-generation DNA sequencing data. Nat. Genet. *43*, 491–498.

Di Cristofano, A., Pesce, B., Cordon-Cardo, C., and Pandolfi, P.P. (1998). Pten is essential for embryonic development and tumour suppression. Nat. Genet. *19*, 348–355.

Ding, Z., Wu, C.-J., Chu, G.C., Xiao, Y., Ho, D., Zhang, J., Perry, S.R., Labrot, E.S., Wu, X., Lis, R., et al. (2011). SMAD4-dependent barrier constrains prostate cancer growth and metastatic progression. Nature *470*, 269–273.

Francis, J.C., Thomsen, M.K., Taketo, M.M., and Swain, A. (2013). β-catenin is required for prostate development and cooperates with Pten loss to drive invasive carcinoma. PLoS Genet. *9*, e1003180.

Gao, D., Vela, I., Sboner, A., Iaquinta, P.J., Karthaus, W.R., Gopalan, A., Dowling, C., Wajala, J.N., Undvall, E.A., Arora, V.K., et al. (2014). Organoid Cultures Derived from Patients with Advanced Prostate Cancer. Cell *158*. Published online September 4, 2014. http://dx.doi.org/10.1016/j.cell.2014.08.016.

Garraway, I.P., Sun, W., Tran, C.P., Perner, S., Zhang, B., Goldstein, A.S., Hahm, S.A., Haider, M., Head, C.S., Reiter, R.E., et al. (2010). Human prostate sphere-forming cells represent a subset of basal epithelial cells capable of glandular regeneration in vivo. Prostate *70*, 491–501.

Goldstein, A.S., Lawson, D.A., Cheng, D., Sun, W., Garraway, I.P., and Witte, O.N. (2008). Trop2 identifies a subpopulation of murine and human prostate basal cells with stem cell characteristics. Proc. Natl. Acad. Sci. USA *105*, 20882–20887.

Grasso, C.S., Wu, Y.-M., Robinson, D.R., Cao, X., Dhanasekaran, S.M., Khan, A.P., Quist, M.J., Jing, X., Lonigro, R.J., Brenner, J.C., et al. (2012). The mutational landscape of lethal castration-resistant prostate cancer. Nature *487*, 239–243.

Hayashi, N., Cunha, G.R., and Parker, M. (1993). Permissive and instructive induction of adult rodent prostatic epithelium by heterotypic urogenital sinus mesenchyme. Epithelial Cell Biol. *2*, 66–78.

Huch, M., Dorrell, C., Boj, S.F., van Es, J.H., Li, V.S., van de Wetering, M., Sato, T., Hamer, K., Sasaki, N., Finegold, M.J., et al. (2013). In vitro expansion of single Lgr5+ liver stem cells induced by Wnt-driven regeneration. Nature *494*, 247–250.

Hudson, D.L., Guy, A.T., Fry, P., O'Hare, M.J., Watt, F.M., and Masters, J.R. (2001). Epithelial cell differentiation pathways in the human prostate: identification of intermediate phenotypes by keratin expression. J. Histochem. Cytochem. *49*, 271–278.

Jung, P., Sato, T., Merlos-Suárez, A., Barriga, F.M., Iglesias, M., Rossell, D., Auer, H., Gallardo, M., Blasco, M.A., Sancho, E., et al. (2011). Isolation and in vitro expansion of human colonic stem cells. Nat. Med. *17*, 1225–1227.

Koo, B.-K., Stange, D.E., Sato, T., Karthaus, W., Farin, H.F., Huch, M., van Es, J.H., and Clevers, H. (2012). Controlled gene expression in primary Lgr5 organoid cultures. Nat. Methods *9*, 81–83.

Lawson, D.A., Xin, L., Lukacs, R.U., Cheng, D., and Witte, O.N. (2007). Isolation and functional characterization of murine prostate stem cells. Proc. Natl. Acad. Sci. USA *104*, 181–186.

Leong, K.G., Wang, B.-E., Johnson, L., and Gao, W.-Q. (2008). Generation of a prostate from a single adult stem cell. Nature *456*, 804–808.

Li, H., and Durbin, R. (2009). Fast and accurate short read alignment with Burrows-Wheeler transform. Bioinformatics *25*, 1754–1760.

Litvinov, I.V., Vander Griend, D.J., Xu, Y., Antony, L., Dalrymple, S.L., and Isaacs, J.T. (2006). Low-calcium serum-free defined medium selects for growth of normal prostatic epithelial stem cells. Cancer Res. *66*, 8598–8607.

Liu, A.Y., Roudier, M.P., and True, L.D. (2004). Heterogeneity in primary and metastatic prostate cancer as defined by cell surface CD profile. Am. J. Pathol. *165*, 1543–1556.

Liu, X., Ory, V., Chapman, S., Yuan, H., Albanese, C., Kallakury, B., Timofeeva, O.A., Nealon, C., Dakic, A., Simic, V., et al. (2012). ROCK inhibitor and feeder cells induce the conditional reprogramming of epithelial cells. Am. J. Pathol. *180*, 599–607.

Luo, W., Rodriguez, M., Valdez, J.M., Zhu, X., Tan, K., Li, D., Siwko, S., Xin, L., and Liu, M. (2013). Lgr4 is a key regulator of prostate development and prostate stem cell differentiation. Stem Cells *31*, 2492–2505.

Marker, P.C., Donjacour, A.A., Dahiya, R., and Cunha, G.R. (2003). Hormonal, cellular, and molecular control of prostatic development. Dev. Biol. *253*, 165–174.

Mehta, V., Abler, L.L., Keil, K.P., Schmitz, C.T., Joshi, P.S., and Vezina, C.M. (2011). Atlas of Wnt and R-spondin gene expression in the developing male mouse lower urogenital tract. Dev. Dyn. *240*, 2548–2560.

Memarzadeh, S., Xin, L., Mulholland, D.J., Mansukhani, A., Wu, H., Teitell, M.A., and Witte, O.N. (2007). Enhanced paracrine FGF10 expression promotes formation of multifocal prostate adenocarcinoma and an increase in epithelial androgen receptor. Cancer Cell *12*, 572–585.

Missol-Kolka, E., Karbanová, J., Janich, P., Haase, M., Fargeas, C.A., Huttner, W.B., and Corbeil, D. (2011). Prominin-1 (CD133) is not restricted to stem cells located in the basal compartment of murine and human prostate. Prostate *71*, 254–267.

Niranjan, B., Lawrence, M.G., Papargiris, M.M., Richards, M.G., Hussain, S., Frydenberg, M., Pedersen, J., Taylor, R.A., and Risbridger, G.P. (2013). Primary culture and propagation of human prostate epithelial cells. Methods Mol. Biol. *945*, 365–382.

Ousset, M., Van Keymeulen, A., Bouvencourt, G., Sharma, N., Achouri, Y., Simons, B.D., and Blanpain, C. (2012). Multipotent and unipotent progenitors contribute to prostate postnatal development. Nat. Cell Biol. *14*, 1131–1138.

Qin, J., Wu, S.-P., Creighton, C.J., Dai, F., Xie, X., Cheng, C.-M., Frolov, A., Ayala, G., Lin, X., Feng, X.-H., et al. (2013). COUP-TFII inhibits TGF-β-induced growth barrier to promote prostate tumorigenesis. Nature *493*, 236–240.

Sato, T., Vries, R.G., Snippert, H.J., van de Wetering, M., Barker, N., Stange, D.E., van Es, J.H., Abo, A., Kujala, P., Peters, P.J., and Clevers, H. (2009). Single Lgr5 stem cells build crypt-villus structures in vitro without a mesenchymal niche. Nature *459*, 262–265.

Sato, T., Stange, D.E., Ferrante, M., Vries, R.G., Van Es, J.H., Van den Brink, S., Van Houdt, W.J., Pronk, A., Van Gorp, J., Siersema, P.D., and Clevers, H. (2011). Long-term expansion of epithelial organoids from human colon, adenoma, adenocarcinoma, and Barrett's epithelium. Gastroenterology *141*, 1762–1772.

Schwank, G., Koo, B.-K., Sasselli, V., Dekkers, J.F., Heo, I., Demircan, T., Sasaki, N., Boymans, S., Cuppen, E., van der Ent, C.K., et al. (2013). Functional repair of CFTR by CRISPR/Cas9 in intestinal stem cell organoids of cystic fibrosis patients. Cell Stem Cell *13*, 653–658.

Shen, M.M., and Abate-Shen, C. (2010). Molecular genetics of prostate cancer: new prospects for old challenges. Genes Dev. *24*, 1967–2000.

Taylor, B.S., Schultz, N., Hieronymus, H., Gopalan, A., Xiao, Y., Carver, B.S., Arora, V.K., Kaushik, P., Cerami, E., Reva, B., et al. (2010). Integrative genomic profiling of human prostate cancer. Cancer Cell *18*, 11–22.

Timms, B.G., Lee, C.W., Aumüller, G., and Seitz, J. (1995). Instructive induction of prostate growth and differentiation by a defined urogenital sinus mesenchyme. Microsc. Res. Tech. *30*, 319–332.

Wang, X., Kruithof-de Julio, M., Economides, K.D., Walker, D., Yu, H., Halili, M.V., Hu, Y.-P., Price, S.M., Abate-Shen, C., and Shen, M.M. (2009). A luminal epithelial stem cell that is a cell of origin for prostate cancer. Nature *461*, 495–500.

Wang, Z.A., Mitrofanova, A., Bergren, S.K., Abate-Shen, C., Cardiff, R.D., Califano, A., and Shen, M.M. (2013). Lineage analysis of basal epithelial cells reveals their unexpected plasticity and supports a cell-of-origin model for prostate cancer heterogeneity. Nat. Cell Biol. *15*, 274–283.

Xin, L., Ide, H., Kim, Y., Dubey, P., and Witte, O.N. (2003). In vivo regeneration of murine prostate from dissociated cell populations of postnatal epithelia and urogenital sinus mesenchyme. Proc. Natl. Acad. Sci. USA *100* (*Suppl 1*), 11896–11903.

Xin, L., Lukacs, R.U., Lawson, D.A., Cheng, D., and Witte, O.N. (2007). Self-renewal and multilineage differentiation in vitro from murine prostate stem cells. Stem Cells *25*, 2760–2769.

Xue, Y., Smedts, F., Debruyne, F.M., de la Rosette, J.J., and Schalken, J.A. (1998). Identification of intermediate cell types by keratin expression in the developing human prostate. Prostate *34*, 292–301.

Yui, S., Nakamura, T., Sato, T., Nemoto, Y., Mizutani, T., Zheng, X., Ichinose, S., Nagaishi, T., Okamoto, R., Tsuchiya, K., et al. (2012). Functional engraftment of colon epithelium expanded in vitro from a single adult Lgr5^{+} stem cell. Nat. Med. *18*, 618–623.